Cooperation and competition determine CD8 T-cell immunodominance hierarchies

Andreas Handel[1] **and Paul Thomas**[2]

[1]Department of Epidemiology and Biostatistics, University of Georgia, Athens, GA

[2]St. Jude Children's Hospital, Memphis, TN

Overview

- Immunodominance, the phenomenon that epitope-specific T-cells expand in a distinct hierarchical fashion, is important for the design of T-cell based intervention strategies.
- We previously used a mathematical model to explain the dynamics of CD8 T-cells specific for the nucleoprotein NP366 and acid polymerase PA224 epitopes during influenza A infections of C57BL/6 mice [1].
- Here, we consider data for additional epitope-specific CD8 T-cell populations (also referred to as cytotoxic T lymphocytes (CTL) in the following). Our previous model, which only included competitive dynamics between CTL populations, fails to explain all experimental observations.
- By extending the model and allowing for cooperative mechanisms between epitope-specific CTL, we are able to fit the data.

We show that a mathematical model that includes both competitive and cooperative mechanisms between epitope-specific CD8 T-cells can describe the immunodominance hierarchies observed in the experimental data.

Mathematical Model

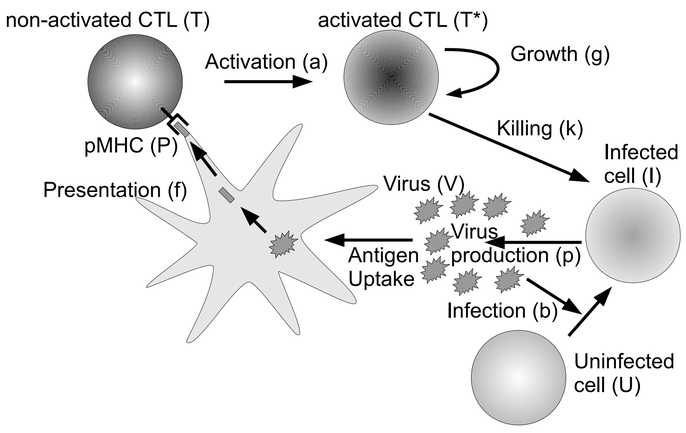

Schematic illustration of the mathematical model. For clarity, the figure does not show the death/decay for virus, infected cells and pMHC. The viral epitopes are presented as epitope-specific peptide-MHC (pMHC), P_i, on activated DC. Antigen presentation increases proportional to virus load with rates f_i and declines at fixed rates, d_i. Unactivated CTL, T_i, are activated by their cognate epitope at rates a_i. Activated CTL, T_i^*, proliferate at rates g_i and kill infected cells at rates k_i.

Model equations and parameters. All parameters are in units of 1/day. The index i labels the different epitopes. Most parameter values are assumed to be the same for the different epitopes.

$$\begin{aligned}
\text{uninfected cells} \quad \dot{U} &= -bUV \\
\text{infected cells} \quad \dot{I} &= bUV - dI - I\sum_i k_i T_i^* \\
\text{virus} \quad \dot{V} &= pI - cV \\
\text{pMHC on activated DC} \quad \dot{P}_i &= f_i V - \delta_i P_i \\
\text{non-activated CTL} \quad \dot{T}_i &= -a_i P_i T_i \\
\text{activated CTL} \quad \dot{T}_i^* &= g_i T_i^* + a_i P_i T_i
\end{aligned}$$

symbol	meaning	value	source
$U(0)$	target cells	10^7	experiment
$V(0)$	initial number of virions	10^5	experiment
$T(0)$	initial naive or memory CTL	fitted	
$I(0)$	infected target cells	0	
$T^*(0)$	activated CTL	0	
b	rate of infection	1×10^{-7}	[2]
d	death rate of infected cell	1	[2–4]
p	production rate of virions	100	[2, 5]
c	virion clearance rate	10	[2, 4]
δ_i	rate of pMHC decay	1	[6]
a_i	rate of CTL activation	10^{-4}	arbitrary
k_i	rate of infected cell killing by CTL	10^{-3}	[7, 8]
g_i	rate of clonal expansion of CTL	0.75	[9, 10]
f_i	rate of pMHC presentation	fitted	

Experiments

8 to 10 week old female B6 mice were initially infected i.p. with 10^8 50% egg infectious doses [EID50]) of H1N1 PR8 virus. After several weeks, the mice were challenged i.n. with 10^6 EID50 of H3N2 x31 virus. Both the wild-type (WT), and "double knockout" (DKO) form of PR8 and x31 virus were given. The DKO viruses are recombinants which lack the NP366 and PA224 epitopes [11]. Virus-specific CD8 T-cell responses were analyzed by flow cytometry at the indicated time post secondary infection. The follwing influenza epitopes were measured: D^{b}NP$_{366-374}$, D^{b}PA$_{224-233}$, K^{b}PB1$_{703-711}$, and D^{b}PB1-F2$_{62-70}$.

The competition model reproduces only some of the data

The figure below shows the best fit of the model to the data. Animals were initially infected with either WT or DKO virus and then challenged with either virus, resulting in four scenarios. CTL numbers on day 8 post secondary infection were measured. The wide hatched bars show the data, the narrow solid smaller bars the model results. For the model, the parameters describing production of pMHC for the different epitopes (f_i) are fitted (for knockout situations, $f_{NP} = f_{PA} = 0$). Also fitted are the initial number naive or memory CTL, assumed to be the same for the different epitopes. All other parameters were fixed to the values listed in the parameter table.

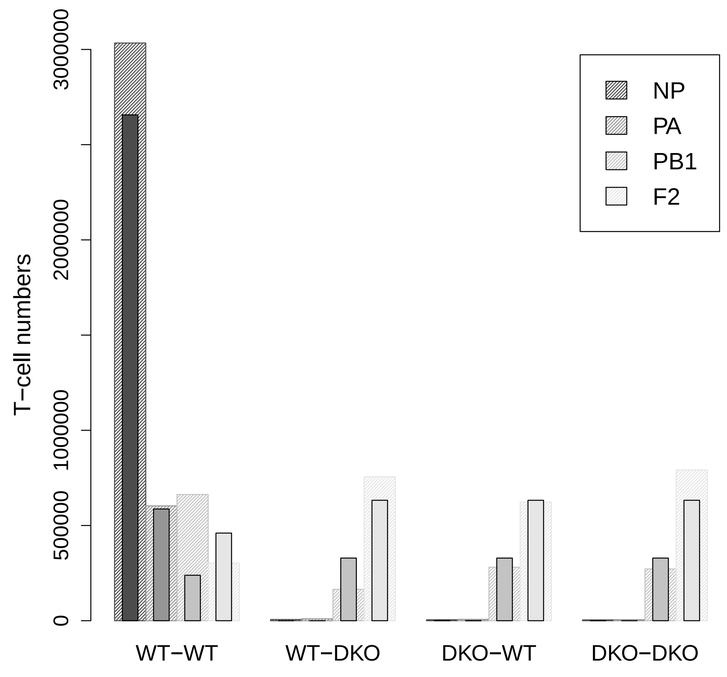

Our model successfully reproduces the competition aspects of the immunodominance dynamics: The removal of NP and PA leads to an increase in the F2 CTL, and the presence of F2 and PB1 memory cells after priming with the DKO virus leads to competitive suppression of the NP and PA CTL during secondary infection (DKO-WT scenario). However, the data also show that removal of the dominant NP and PA epitopes leads to a **decreased** response for the PB1 CTL. This feature can not be captured with the model described above, even if we fit instead of fix the remaining parameters (not shown). This calls for an extended model, which we describe next.

Extended model with cooperation

The decrease in the PB1 response after removal of the NP and PA epitopes can be explained through a cooperation mechanism. One such mechanism could envolve cytokine production. T-cells need cytokines such as IL-2 for optimal division and they also produce these cytokines. It is plausible that the removal of the NP and PA CTL populations leads to suboptimal cytokine levels for the other responding CTL populations and therefore suboptimal growth. This could be modelled by making the growth rate of the CTL dependent on the total number of CTL, i.e.

$$g_i \rightarrow \frac{g_i T_{tot}}{T_{tot} + s_i}, \tag{1}$$

where T_{tot} is the total number of activated CTL. If there are few CTL ($T_{tot} \ll s_i$), those CTL expand at a rate $\approx g_i T_{tot}/s_i$, which can be much lower than the expansion rate g_i at high CTL numbers ($T_{tot} \gg s_i$). Therefore, if the overall number of CTL is low because for instance the NP and PA CTL do not get activated, it could lead to a reduced expansion of the PB1 population.

The extended model can reproduce the data

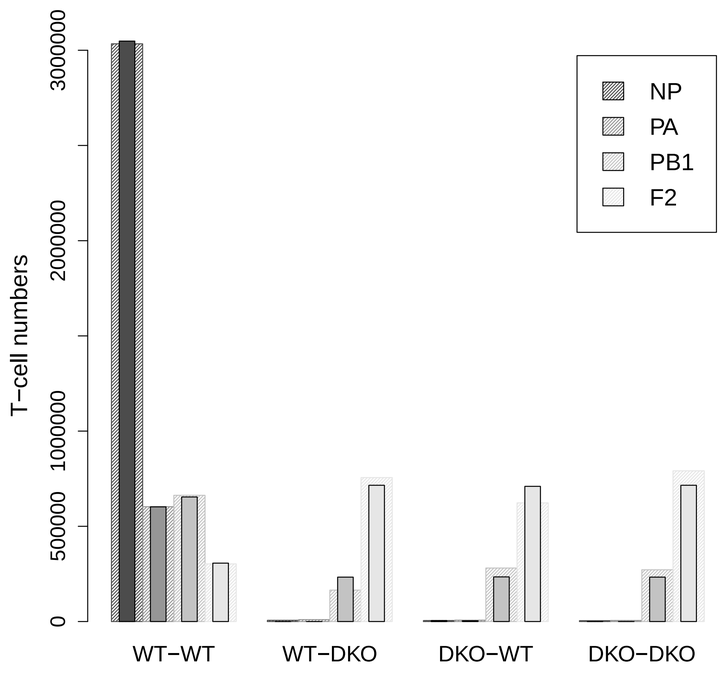

We now fit the extended model to the data. We again fit the parameters f_i and the initial number of naive/memory CTL. In addition, we fit the s_i for the four different epitopes. As the figure shows, the model can reproduce the data. Removal of NP and PA leads now to an increased F2 but decreased PB1 response. The different behaviors of the PB1 and F2 CTL are encompassed by their different dependence on the total CTL population (cytokines), expressed by $s_{PB1} \gg s_{F2}$.

Discussion and Future Steps

- Combining experiments with quantitative dynamical models can be useful for understanding the complex, multi-factorial processes that lead to immunodominance in particular and that govern the infection dynamics in general.
- Alternative competition mechanisms (e.g. killing of DC, competition for antigen) are possible.
- Equivalently, different cooperation mechanisms (e.g. pMHC presentation, CTL activation) are possible.
- A number of those alternative mechanisms/models can also reproduce the current data (not shown).
- The different mechanisms/models make different predictions for certain scenarios, which we can/will test experimentally.
- Measuring more variables of the model (e.g. pMHC, virus load) will either provide further support for specific models or rule out some currently plausible models.

References

[1] Handel, A. & Antia, R. A simple mathematical model helps to explain the immunodominance of CD8 T cells in influenza A virus infections. *J Virol* **82**, 7768–7772, Aug (2008).

[2] Beauchemin, C. A. A. *et al.* Modeling amantadine treatment of influenza A virus in vitro. *J Theor Biol* **254**, 439–451, Sep (2008).

[3] Brydon, E. W. A., Smith, H. & Sweet, C. Influenza A virus-induced apoptosis in bronchiolar epithelial (NCI-H292) cells limits pro-inflammatory cytokine release. *J Gen Virol* **84**, 2389–2400, Sep (2003).

[4] Baccam, P., Beauchemin, C., Macken, C. A., Hayden, F. G. & Perelson, A. S. Kinetics of influenza A virus infection in humans. *J Virol* **80**, 7590–7599, Aug (2006).

[5] HORSFALL, F. L. Reproduction of influenza viruses; quantitative investigations with particle enumeration procedures on the dynamics of influenza a and b virus reproduction. *J Exp Med* **102**, 441–473, Oct (1955).

[6] Belz, G. T., Zhang, L., Lay, M. D. H., Kupresanin, F. & Davenport, M. P. Killer T cells regulate antigen presentation for early expansion of memory, but not naive, CD8+ T cell. *Proc Natl Acad Sci U S A* **104**, 6341–6346, Apr (2007).

[7] Yates, A. *et al.* Revisiting Estimates of CTL Killing Rates In Vivo. *PLoS ONE* **2**, e1301 (2007).

[8] Ganusov, V. V. & Boer, R. J. D. Estimating in vivo death rates of targets due to cd8 t-cell-mediated killing. *J Virol* **82**, 11749–11757, Dec (2008).

[9] Belz, G. T., Xie, W. & Doherty, P. C. Diversity of epitope and cytokine profiles for primary and secondary influenza a virus-specific CD8+ T cell responses. *J Immunol* **166**, 4627–4633, Apr (2001).

[10] Legge, K. L. & Braciale, T. J. Lymph node dendritic cells control CD8+ T cell responses through regulated FasL expression. *Immunity* **23**, 649–659, Dec (2005).

[11] Webby, R. J. *et al.* Protection and compensation in the influenza virus-specific CD8+ T cell response. *Proc Natl Acad Sci U S A* **100**, 7235–7240, Jun (2003).

This work is supported by grants from the NIH